

Anomalous Diamagnetic Susceptibility in 13-Atom Platinum Nanocluster Superatoms**

Emil Roduner,* Christopher Jensen, Joris van Slageren, Rainer A. Rakoczy, Oliver Larlus, and Michael Hunger

Abstract: We are used to being able to predict diamagnetic susceptibilities χ_D to a good approximation in atomic increments since there is normally little dependence on the chemical environment. Surprisingly, we find from SQUID magnetization measurements that the χ_D per Pt atom of zeolite-supported Pt_{13} nanoclusters exceeds that of Pt^{2+} ions by a factor of 37–50. The observation verifies an earlier theoretical prediction. The phenomenon can be understood nearly quantitatively on the basis of a simple expression for diamagnetic susceptibility and the superatom nature of the 13-atom near-spherical cluster. The two main contributions come from ring currents in the delocalized hydride shell and from cluster molecular orbitals hosting the Pt 5d and Pt 6s electrons.

Nanosize particles of metallic elements have attracted great attention because their properties often deviate markedly from those of the bulk metal. For example, micro- and nanosize platinum particles are reported to become superconducting,^[1–3] whereas bulk Pt does not. There are predictions that metal clusters with 10^2 – 10^3 free carriers may become superconducting.^[4] Furthermore, at low temperature, Pt nanoparticles and clusters show pronounced superparamagnetism,^[5–7] whereas bulk Pt has a small positive magnetic susceptibility arising from Pauli paramagnetism which is slightly temperature dependent.^[8] Other work predicts a greatly enhanced diamagnetism in metal clusters,^[9,10] but there has been no experimental verification of this. Diamagnetism is an important indicator of superconductivity as well, which raises the interest in this property for small clusters even further. However, since the London penetration depth of superconductors is normally on the order of 100 nm it

should not be expected to find an ideal diamagnetism with full exclusion of the magnetic field for objects of less than 1 nm diameter. In addition, since magnetic properties reflect the wave function they are of general interest in physics as well as in chemistry.

We have previously demonstrated that monodisperse icosahedral or cuboctahedral platinum nanoclusters with 13 ± 2 atoms can be prepared supported within the porous structure of NaY zeolite.^[6] Although they are all of the same size they exist in three different magnetic states: 15–20 % in a high-spin state with magnetic moments of $\mu = 3.7 \pm 0.4$ and $3.0 \pm 0.4 \mu_B$ for $[Pt_{13}]$ and $[Pt_{13}H_m]$, respectively, a very small fraction, less than 1 %, contributes to the spin- $1/2$ EPR signal, and the rest is diamagnetic.^[7] The coexistence of different electronic states of the same cluster may be rationalized by different local environments, such as the presence of different numbers of zeolite framework Al atoms or extra-framework cations, Na^+ or K^+ , in close proximity to the cluster, and the extent of hydrogen coverage will also play a role.

Herein we resume the subject of magnetism with these clusters using a specially synthesized iron-free L zeolite (Supporting Information) to avoid any interference of iron and ambiguities in the interpretation of the data. The potassium form of the zeolite was exchanged using a 3 mM solution of $[Pt(NH_3)_4]Cl_2$. The product was washed, dried, and then calcined in a flux of O_2 while the sample was heated at a rate of $0.5 K min^{-1}$, and keeping the final temperature (623 K) for 5 h. Reduction was then performed in flowing H_2 at a heating rate of $4 K min^{-1}$ and keeping the sample at 503 K for 1 h. The structure of the obtained zeolite sample was characterized by X-ray diffraction and solid-state NMR spectroscopy (see Supporting Information, Figure S1 and S2), while the investigation of the Pt clusters was performed by extended X-ray absorption fine structure (EXAFS)^[6,11] and EPR spectroscopy. Details about the experimental procedure which are crucial for formation of clusters of a defined size are found elsewhere.^[12,13] The extent of H_2 or D_2 coverage was determined by sequential addition of calibrated hydrogen aliquots and monitoring the pressure.^[11]

The EPR spectrum of a $[Pt_{13}D_x]$ cluster shows a multiplet spectrum with a regular splitting (see Figure S3). The pattern fits well the hyperfine interaction of the unpaired electron with 12 equivalent Pt nuclei in natural isotopic abundance and suggests a superatom structure (Supporting Information). The resolved multiplet is clear evidence for a molecular rather than metallic character of the cluster.

Magnetization measurements were performed with a $[Pt_{13}H_{38}]$ and a $[Pt_{13}H_{18}]$ sample using a superconducting quantum interference device (SQUID, quantum design

[*] Prof. E. Roduner, Dr. C. Jensen, Prof. J. van Slageren
Institute of Physical Chemistry, University of Stuttgart
70563 Stuttgart (Germany)

E-mail: E.Roduner@ipc.uni-stuttgart.de

Dr. R. A. Rakoczy, Dr. O. Larlus
Clariant Produkte Deutschland GmbH
Lenbachplatz 6, 80333 Munich (Germany)

Prof. M. Hunger
Institute of Technical Chemistry, University of Stuttgart
70563 Stuttgart (Germany)

Prof. E. Roduner
University of Pretoria
0002 Pretoria (Republic of South Africa)

[**] We thank Hermann Stoll for useful discussions and the 1st Physical Institute of the University of Stuttgart for letting us use their SQUID magnetometer.

Supporting information for this article is available on the WWW under <http://dx.doi.org/10.1002/anie.201310637>.

MPMXL7). Paramagnetism was discussed in detail in Ref. [12]. In short, Curie behavior with a Curie–Weiss constant $\theta=0$ was observed in a temperature range of 20–70 K. A magnetic moment of $0.236(2) \mu_B$ per Pt atom was obtained for both samples,^[13] corresponding to $J \approx 1.5$ for the 13-atom cluster or three unpaired electrons if the moment is due to electron moments only. These values oscillate significantly with the amount of chemisorbed hydrogen, and they show some development with time.^[12,13] Previous XMCD (X-ray magnetic circular dichroism) measurements of two similar samples with not quantitatively known hydrogen coverage revealed a ratio of orbital to spin magnetic moments, m_L/m_S of $0.30(2)$, and thus to an orbital angular momentum contribution to paramagnetism of approximately 23 %, significantly less than for bulk Pt (28 %).^[7]

The magnetization saturation curves shown in Figure 1 A reveal the paramagnetic nature of the samples owing to a fraction of high-spin clusters at low temperature. All magnetizations are corrected for the contribution of the plain zeolite. At room temperature and fields greater than 0.2 T, however, the magnetizations turn negative, scaling linearly with field, so the behavior is clearly dominated by diamagnetism.

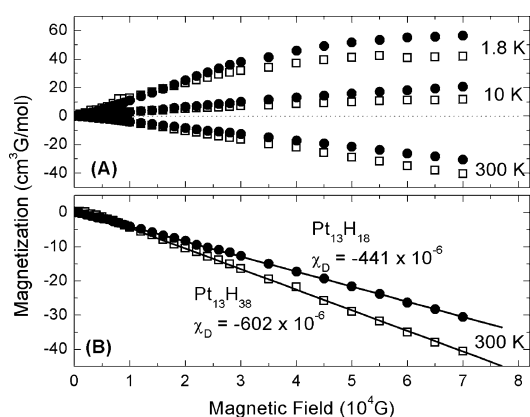


Figure 1. SQUID magnetization measurements obtained with 5.5 wt. % Pt supported on iron-free KL-zeolite for A) $[\text{Pt}_{13}\text{H}_{18}]$ (full dots) and $[\text{Pt}_{13}\text{H}_{38}]$ (empty squares) and B) for 300 K on an expanded scale. The magnetization of the same amount of zeolite in the absence of Pt was subtracted. The numbers are given per mol Pt atoms.

Above 40 K, the EPR signal diminishes much more quickly than predicted by the Curie law, indicating that a chemical equilibrium is also involved.^[14] If this is also true for the high-spin state then it is not surprising that nearly no influence of the paramagnetic fraction is observed at 300 K. Elsewhere, it was demonstrated for the 13-atom clusters Mn@Sn_{12} that excitation of Jahn–Teller active vibrations has a pronounced effect on the spin structure and causes rapid transitions between states.^[15] Evidence for the excitation of vibrations at low frequencies as expected for the heavy-atom Pt clusters comes from the relaxation rate of the $[\text{Pt}_{13}\text{D}_x]$ EPR signal which increases with the square of temperature.^[14]

The raw data of the field-dependent magnetization measurements are given in Figure S4, together with an

explanation of the subtraction of the zeolite contribution. The slopes of the resulting straight lines in Figure 1 B are the molar magnetic susceptibilities, in cgs units, given by $\chi_D = -441(1) \times 10^{-6} \text{ cm}^3$ and $\chi_D = -602(4) \times 10^{-6} \text{ cm}^3$ per mol Pt atoms of $[\text{Pt}_{13}\text{H}_{18}]$ and $[\text{Pt}_{13}\text{H}_{38}]$, respectively. The latter sample is saturated with hydrogen at a pressure of 540 mbar.^[11] These values are spectacular, larger by as much as a factor of 37–50 compared with expected values for non-metallic diamagnetic Pt [$\chi_D(\text{Pt}) \approx 2\chi_D(\text{PtCl}_2) - \chi_D(\text{PtCl}_4) = -11 \times 10^{-6} \text{ cm}^3 \text{ mol}^{-1}$; or $\chi_D(\text{Pt}) \approx \chi_D(\text{PtCl}_2) - \chi_D(\text{Cl}_2) = -13.5 \times 10^{-6} \text{ cm}^3 \text{ mol}^{-1}$].^[16]

All Pt species contribute to the diamagnetic susceptibility. The origin of this property is normally attributed to ring currents on atoms which lead to a magnetic moment that is antiparallel to the external magnetic field (Figure 2). It is

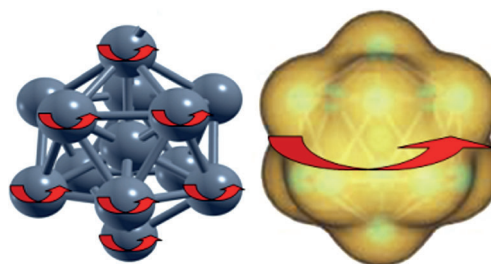


Figure 2. The mechanism of diamagnetism is ascribed to magnetic-field-induced ring currents which are localized on the atoms and lead to a small magnetic moment that scales with the square of the radius and is antiparallel to the external magnetic field (left). Owing to the superatom nature of clusters, the ring current operates in the delocalized valence orbitals (right). The strongly enhanced diamagnetism is due to the cluster radius and the large number of electrons involved.

analogous to the mechanism which is responsible for the large diamagnetic screening in the proton NMR spectrum of benzene. For a closed-shell cluster consisting of N atoms electron-spin paramagnetism and orbital diamagnetism vanish, and the dimensionless volume susceptibility χ is given to first order in SI units by Equation (1)^[17]

$$\chi = -\frac{e^2 \mu_0 N}{6m_e V} \sum_i \langle r_i^2 \rangle \quad (1)$$

where μ_0 is the vacuum permeability, and e and m_e are the electron charge and mass, respectively. V is the atomic volume, 0.0152 nm^3 based on the bulk density of Pt, and $\langle r_i^2 \rangle$ is the mean square electron distance of the i -th electron from the center. To convert Equation (1) into molar susceptibilities χ_m , χ has to be multiplied by the molar volume, $9.09 \text{ cm}^3 \text{ mol}^{-1}$, and to convert into the more conventional cgs units χ_D in which all values are quoted herein, it has to be divided by 4π . In atoms, $\langle r_i^2 \rangle$ is on the order of a_0^2 , where a_0 is the Bohr radius. The ground-state electron configuration of Pt is $[\text{Xe}]4f^{14}5d^96s^1$.

In the superatom picture it will be the delocalized cluster molecular orbitals which determine diamagnetism. These provide larger radii for the ring currents (see Figure 2), but it

Table 1: Diamagnetic susceptibility χ_D of $[\text{Pt}_{13}\text{H}_x]$ clusters in units of 10^{-6} cm^3 per mol Pt atoms.

Sample	Calculated contribution (number of electrons)				sum	Experimental value
	(i) $[\text{Xe}]4f^{14}$ core ^[b]	(ii) Hydride shell ^[c]	(iii) 5d6s shell ^[a] Overall Pt_{13} cluster	(iv) 5d6s shell ^[a] Pt_4 tetrahedra		
$[\text{Pt}_{13}\text{H}_{38}]$	−12	−313 (76/13)	−135 ((120−38)/13)	−62 ((40−38−3/12)/4)	−522	−602(4)
$[\text{Pt}_{13}\text{H}_{18}]$	−12	−148 (36/13)	−167 ((120−18)/13)	−72 ((40−18−3/12)/4)	−399	−441(1)
$[\text{Pt}_{13}]$	−12	0	−200 (120/13)	−81 (40/4)	−293	Not measured

[a] Ten 5d and 6s electrons for each of the 12 surface Pt atoms, diminished by the number of electrons which are involved in the Pt–H bonds, (i)–(iv) refer to the description of the contributions in the main text. χ_D is given per atom of the 13-atom cluster. [b] Approximate experimental value for Pt^{2+} , see text. The number should be diminished slightly through the atomic contribution of the remaining eight d electrons which are part of the 5d6s superatom shell. [c] Two electrons per Pt–H bond.

appears nevertheless challenging to explain the experimental enhancement by a factor 37–50, depending on hydrogen coverage. In addition to the conventional atomic values (i, see Table 1) we discuss three possible further contributions: ii) Surprisingly, it was found necessary to involve the shell of chemisorbed hydrogen atoms. The 1s atomic orbital of H is energetically significantly lower than the 5d orbital of Pt to which it is bound. The Pt–H bonding orbital will thus also be of low energy, about 5 eV below the Fermi level, making H partly hydride-like (the antibonding orbital is slightly above the Fermi level^[18]). In DFT quantum chemical calculations the bridge-bonded site along the cluster edge was predicted the most stable, but this is without any corrections for zero-point vibrational motion, and the difference to the on-top Pt and the threefold hole sites is not large.^[14,19] The H–H distance of saturated Pt clusters amounts to about 0.22 nm or $4.7a_0$.^[19] At this distance there is considerable overlap of the H 1s electrons, in particular in the hydridic state, which justifies regarding the Pt bound hydrides as a set of doubly occupied delocalized cluster molecular orbitals.^[19] Approximating the radial distance of this shell from the cluster center by the sum of the Pt–Pt and the Pt–H bond lengths ($0.277 \text{ nm} + 0.158 \text{ nm} = 0.435 \text{ nm}$) we arrive at a contribution to χ_D of $-53.5 \times 10^{-6} \text{ cm}^3$ per mol hydride electrons. Per Pt atom this yields $\chi_D = -148 \times 10^{-6} \text{ cm}^3$ for $[\text{Pt}_{13}\text{H}_{18}]$, and $-313 \times 10^{-6} \text{ cm}^3$ for $[\text{Pt}_{13}\text{H}_{38}]$. iii) The next contribution is due to the delocalized Pt valence electrons. r_i is the positive cluster core radius, which is taken in this case as the bulk Pt interatomic distance, $d = 0.277 \text{ nm}$.^[20] On this basis we obtain $\chi_D = -21.6 \times 10^{-6} \text{ cm}^3$ per mol valence electrons. iv) Induced ring currents cannot only extend over the entire cluster, but also over smaller building blocks. A 13-atom cuboctahedron consists of one central atom surrounded by six atoms in one plane. Three adatoms are found on top and three more below this plane. This structure can be thought of as being composed of six edge-sharing Pt_4 tetrahedra, three pointing up from the central plane and three down. The four atoms sit on a sphere with a radius $R = 0.25 \cdot 6^{1/2} d$, leading to an increment $\chi_D = -8.1 \times 10^{-6} \text{ cm}^3$ per mol valence electrons.

There are also 14 4f electrons per atom. If they were delocalized over the cluster this would lead to a contribution of the required magnitude. However, they are energetically lower by 73 eV than the 5d and 6s electrons and have an atomic $\langle r^2 \rangle$ expectation value of only $0.3a_0^2$, an order of magnitude less than the 4d electrons.^[21] This situation leaves them little probability of overlap and delocalization, so they

will contribute only to the atomic core values. Indeed, they are not normally regarded as valence orbitals.

The four contributions to χ_m are collected in Table 1. Contribution (iv) of the Pt_4 tetrahedra appears to be minor but non-negligible. Furthermore, for icosahedra in place of cuboctahedra the building blocks would have to be constructed differently. The added contributions account for 87 % of the experimental value for $[\text{Pt}_{13}\text{H}_{38}]$ and to 90 % for $[\text{Pt}_{13}\text{H}_{18}]$. The predicted values are somewhat low, but considering the extensive and debatable approximations in the model the results are still considered to be in perhaps very good qualitative agreement with experiment. The advantage of the model is that it provides insight into the possible mechanism of diamagnetism in nanoparticles. Detailed quantum chemical predictions would be highly desirable, but such calculations seem currently to be out of range for a heavy element such as Pt, for which relativistic effects are crucial.

The SQUID results represent an ensemble average over all the Pt species, but potential size and shape inhomogeneities are expected to play a limited role for the diamagnetism. The agreement between theoretical model and experimental result suggests that the observed phenomenon has nothing to do with a superconducting transition, even though the clusters have 10^2 – 10^3 delocalized electrons.^[4] Since the EPR multiplet confirms that the clusters are non-metallic this also excludes other origins, such as a negative Knight shift. Instead, we believe that this is the first experimental observation of the predicted anomalously enhanced diamagnetic susceptibility in a well-defined finite-size delocalized system.

A superatom shell-type electronic structure has also been predicted in density functional calculations for Pt_{13} clusters which did not include any chemisorbed hydrogen atoms.^[22] The present essentially quantitative agreement strongly supports that the superatom concept provides a useful description for understanding small spherical clusters. Both, this concept and the strongly enhanced diamagnetism are characteristic and unique for nanomaterials with delocalized electron systems.

It would be interesting to investigate the transition to bulk behavior which has been predicted to occur at a nanoparticle size with a radius on the order of $10 \mu\text{m}$.^[10]

Received: December 8, 2013

Revised: January 27, 2014

Published online: March 18, 2014

Keywords: diamagnetism · EPR spectroscopy · platinum clusters · superatoms

- [1] R. König, A. Schindler, T. Herrmannsdörfer, *Phys. Rev. Lett.* **1999**, *82*, 4528–4530.
- [2] A. Schindler, R. König, T. Herrmannsdörfer, H. F. Braun, *Phys. Rev. B* **2000**, *62*, 14350–14358.
- [3] A. Schindler, R. König, T. Herrmannsdörfer, H. F. Braun, G. Eska, D. Günther, M. Meissner, M. Mertig, R. Wahl, W. Pompe, *Physica B* **2003**, *329–333*, 1427–1428.
- [4] V. Z. Kresin, Yu. N. Ovchinnikov, *Physics Uspekhi* **2008**, *51*, 427–435.
- [5] Y. Yamamoto, T. Miura, Y. Nakae, T. Teranishi, M. Miyake, H. Hori, *Physica (Amsterdam)* **2003**, *329B–333B*, 1183–1184.
- [6] X. Liu, M. Bauer, H. Bertagnolli, E. Roduner, J. van Slageren, F. Phillipp, *Phys. Rev. Lett.* **2006**, *97*, 253401; X. Liu, M. Bauer, H. Bertagnolli, E. Roduner, J. van Slageren, F. Phillipp, *Phys. Rev. Lett.* **2009**, *102*, 049902.
- [7] J. Bartolomé, F. Bartolomé, L. M. Garcia, E. Roduner, Y. Akdogan, F. Wilhelm, A. Rogalev, *Phys. Rev. B* **2009**, *80*, 014404.
- [8] J. E. Dam, P. C. M. Gubbens, G. J. van den Berg, *Physica* **1973**, *70*, 520–546.
- [9] A. I. Buzdin, O. V. Dolgov, Yu. E. Lozovik, *Phys. Lett. A* **1984**, *100*, 261–263.
- [10] V. Kresin, *Phys. Rev. B* **1988**, *38*, 3741–3746.
- [11] C. Jensen, D. Buck, H. Dilger, M. Bauer, F. Phillipp, E. Roduner, *Chem. Commun.* **2013**, *49*, 588–590, see also the Supporting Information.
- [12] C. Jensen, J. van Slageren, P. Jakes, R.-A. Eichel, E. Roduner, *J. Phys. Chem. B* **2013**, *117*, 22732–22745.
- [13] C. Jensen, PhD thesis, University of Stuttgart, 2013. http://elib.uni-stuttgart.de/opus/volltexte/2013/8361/pdf/Diss_Jensen.pdf.
- [14] X. Liu, H. Dilger, R. A. Eichel, J. Kunstmann, E. Roduner, *J. Phys. Chem. B* **2006**, *110*, 2013–2023.
- [15] U. Rohrmann, R. Schäfer, *Phys. Rev. Lett.* **2013**, *111*, 133401.
- [16] *CRC Handbook of Chemistry and Physics*, 55th ed., CRC Press, Cleveland, OH, **1974–1975**.
- [17] S. Blundell, *Magnetism in Condensed Matter, Oxford Masters Series in Condensed Matter Physics*, Oxford University Press, Oxford, **2001**.
- [18] B. Hammer, J. K. Nørskov, *Nature* **1995**, *376*, 238–240.
- [19] L. Chen, C. Zhou, J. Wu, H. Cheng, *Front. Phys. China* **2009**, *4*, 356–366.
- [20] N. Watari, S. Ohnishi, *Phys. Rev. B* **1998**, *58*, 1655–1677.
- [21] J. P. Desclaux, *At. Data Nucl. Data Tables* **1973**, *12*, 311–406.
- [22] N. Watari, S. Ohnishi, *J. Chem. Phys.* **1997**, *106*, 7531–7540.